

# Cystine calculi: correlation of CT-visible structure, CT number, and stone morphology with fragmentation by shock wave lithotripsy

Samuel C. Kim · Erin K. Burns · James E. Lingeman ·  
Ryan F. Paterson · James A. McAteer ·  
James C. Williams Jr

Received: 12 June 2007 / Accepted: 9 October 2007 / Published online: 27 October 2007  
© Springer-Verlag 2007

**Abstract** Cystine stones are often highly resistant to shock wave lithotripsy (SWL), but it has been reported that cystine stones of “rough” morphology are actually quite susceptible to SWL. Based on the observation that rough cystine stones contain void regions that are visible by helical computed tomographic (CT) imaging, we hypothesized that the internal structure of cystine stones would correlate with the susceptibility of stones to SWL. Cystine stones with average diameters between 4 and 7 mm were scanned using micro and helical CT, classified morphologically according to published criteria, and broken in a research electrohydraulic lithotripter, with fragments sieved through a 2 mm mesh every 50 SWs. Stones with regions of low X-ray attenuation visible on helical CT required only  $650 \pm 312$  SW/g for total comminution, while those that did not show CT-visible internal structure required  $1,046 \pm 307$  SW/g (mean  $\pm$  SD,  $P < 0.004$ ). In addition, both average and minimum values for CT number (in Hounsfield units, HU) correlated with SW/g to comminution ( $P < 0.003$  and  $P < 0.0003$ , respectively), and these relationships were independent of stone size. This study also confirmed the relationship between the morphological criteria of Bhatta et al. (J Urol 142:937–940, 1989) and cystine stone fragility: Rough stones required  $609 \pm 244$  SW/g ( $n = 11$ ), smooth stones  $1,109 \pm$

$308$  SW/g ( $n = 8$ ), and stones intermediate in morphology  $869 \pm 384$  SW/g ( $n = 7$ ; rough different from smooth,  $P < 0.005$ ). In conclusion, cystine stones that appeared homogeneous by helical CT required 61% more SWs for comminution than did stones showing regions of low X-ray attenuation. These findings demonstrate the feasibility of using helical CT to identify cystine stones that will be susceptible to SWL.

**Keywords** Cystine · Computed tomography · Attenuation values · Shock wave lithotripsy

## Introduction

Cystine calculi have long been considered to be resistant to treatment using shock wave lithotripsy (SWL) [1–11], and while SWL can be effective for many cystine stones, it would be useful to be able to predict which stones can be successfully treated with SWL [12]. It is also recognized that all cystine stones do not exhibit the same morphology [13], and Bhatta et al. [14] reported in 1989 that cystine stones with a “rough” morphology (having large, blocky crystals at their surface) broke more easily with SWs than did cystine stones with “smooth” morphology (smaller crystals at the surface, and with paler color). Unfortunately, the surface roughness and color of patient stones are not qualities that can be assessed at diagnosis [15].

Non-contrast helical CT is the standard for imaging patient stones before treatment [16], so this is the logical methodology to explore the possibility that the structural features of cystine stones can be used to predict their fragility. In a previous report, we showed that rough cystine stones possess void regions within them that make them distinctive by helical CT [17]. In the present study, we

S. C. Kim · J. E. Lingeman · R. F. Paterson  
Methodist Hospital Institute of Kidney Stone Disease,  
Indiana University School of Medicine and Indiana Kidney  
Stone Institute, Indianapolis, IN, USA

E. K. Burns · J. A. McAteer · J. C. Williams Jr (✉)  
Department of Anatomy and Cell Biology, Indiana University  
School of Medicine, 635 Barnhill Drive, MS 5035,  
Indianapolis, IN 46202, USA  
e-mail: williams@anatomy.iupui.edu

measured SWL fragility in cystine stones and looked for correlations with CT-visible structure and with CT number. The results suggest that fragile cystine stones have structural characteristics that are detectable by helical CT, so that identification of such stones is clinically feasible.

## Methods

Cystine calculi were obtained as patient discards locally (from Beck Analytical Services, Indianapolis, IN), and from the Department of Urology at Northwestern University (Chicago, IL, courtesy of Dr. Robert Nadler) and the Laboratory for Stone Research (Newton, MA, courtesy of Dr. Edwin Prien). Stones came de-identified, so it was not known how many stones from a given site might have come from the same patient. Stones were analyzed non-destructively using an mCT20 Micro CT scanner (Scanco Medical, Switzerland) using voxel sizes ranging from 20 to 34  $\mu\text{m}$ . Stone content of cystine was confirmed using micro CT X-ray attenuation values [18], and total stone volumes were determined. From each stone volume, an average stone diameter was calculated.

Stones were classified morphologically by the system of Bhatta et al. [14]. Rough cystine stones were observed to be composed of large crystals, while smooth stones were composed of small crystals, and also tended to have a lighter color than did rough stones. Some stones were classified as “intermediate” in type, having regions with both rough and smooth morphologies, or being composed of crystals of sizes in between those seen for rough and smooth stones. None of the rough stones were large in size, so the upper stone diameter limit for this study was taken to be 7 mm, which was just greater than the largest rough stone (6.9 mm). The lower limit of stone size for the study was taken to be 4 mm, a diameter that can sometimes be clinically significant. Thus, morphologically, the stones consisted of three classes, with stone sizes not differing among rough (11 stones,  $5.5 \pm 0.9$  mm), intermediate (7 stones,  $5.3 \pm 0.9$  mm), and smooth cystine stones (8 stones,  $6.0 \pm 0.3$  mm).

Helical CT was performed on all stones in vitro using a clinical 4-head General Electric Quad Scanner (80 kV, 80 mA, 1.25 mm collimation, pitch 0.938:1). Stones were scanned dry in 15 ml polypropylene centrifuge tubes, packed with cotton gauze. Bone windows were used for image viewing as previously described [19]. Attenuation values were obtained for stones by drawing a representative elliptical region of interest (ROI) in the HCT slice with the largest diameter. The ROI was drawn excluding the outer rim of the stone to decrease volume-averaging errors [20]. Mean, maximum, and minimum attenuation values were recorded. Stones were also graded for visibility of

regions of low attenuation (internal voids) by an observer blinded as to the morphological classifications of the stones. Examples of helical CT images are shown in Fig. 1.

Lithotripsy was performed on the cystine stones in a research lithotripter modeled after the Dornier HM3 [21]. Stones were hydrated for 96 h in citric acid buffer (pH = 3.0, chosen to minimize dissolution of the stones). Each electrode was conditioned with 100 SWs and the maximum number of SWs delivered by an electrode was 2,000. SWs were delivered 50 at a time, at 20 kV and 1 Hz; after each 50-SW dose, the stone material was sieved through a 2 mm mesh, and fragments retained on the mesh were returned to the lithotripter for another 50-SW dose. This process was repeated until all of the fragments were able to pass through the mesh. Fragments passed through the sieve were rinsed with deionized water, dried overnight, weighed, and the percentage of fragments for each 50-SW dose was calculated using the total weight of recovered fragments as the denominator. The total number of SWs delivered to each stone was taken as the SWs to comminution, and this number was normalized to stone size using weight [22]. This method of assessing SW fragility was used on account of the precious nature of the cystine stones being comminuted. In the past, we have used either a fixed dose of SWs or SWs to total comminution as measures of stone fragility, but these methods do not measure exactly the same properties of stones [23]. The method used in the present study essentially combines the fixed-dose and SWs-to-total-comminution methods, and was used so that these hard-to-find stones could be studied in a way that would guarantee a good measure of fragility to lithotripter SWs.

Data were compared using *t* tests, the Tukey–Kramer HSD test, or linear regression as appropriate; differences were considered significant at  $P < 0.05$ . Data are expressed as mean  $\pm$  SD, except where noted otherwise. Fitting to the 50-SW data was done assuming an exponential relationship between the percentage of the stone that had been broken ( $f$ ), and the number of SWs delivered ( $N$ ):

$$f = 100 \left( 1 - e^{-\frac{N \ln(0.5)}{N_{1/2}}} \right)$$

where  $N_{1/2}$  is the number of SWs to half-comminution (50%), the “half-life” of the stone during its exposure to SWs. The fitting of the data to determine  $N_{1/2}$  values was accomplished using the nonlinear fitting platform of JMP IN 5.1 (SAS Institute, Cary, NC, USA). Comparison of groups was done using confidence intervals based on the likelihood method;  $P < 0.001$  indicates that the  $\alpha = 0.001$  confidence intervals for  $N_{1/2}$  for groups were non-overlapping.

Note that this nonlinear method is extremely sensitive to stone size, as it will usually take more SWs to break a large stone than it will for a small stone. We know of no obvious



**Fig. 1** Typical images of cystine stones using helical CT

way to normalize the method to stone size, as is more easily done with SWs to total comminution (see below). However, if stone size is well controlled, this method can provide a superior way to distinguish small differences in fragility.

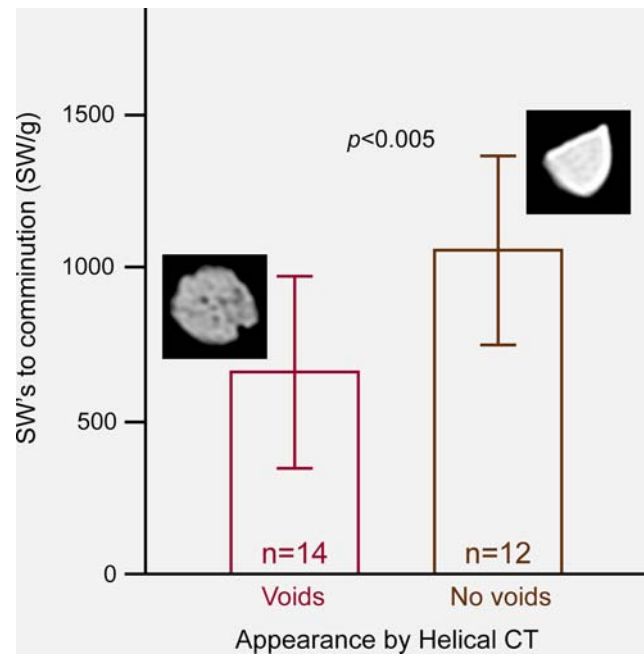


**Fig. 2** Shock waves to complete comminution, normalized to stone weight, for cystine stones grouped using helical CT, as shown in Fig. 1

## Results

Cystine stones that showed void regions by helical CT were significantly more fragile to SWs than were cystine stones that were judged to be homogeneous by CT (Fig. 2). Homogeneous stones required an average of 1,046 SWs/g, while those with visible void regions required only 650 SWs/g. These groups of stones did not differ by size, being of  $5.7 \pm 0.9$  and  $5.5 \pm 0.8$  mm average diameter, respectively.

The data were also analyzed using an exponential fit to the 50-SW data, as shown in Fig. 3. This method yields an average value for the number of SWs to half-comminution for the groups,  $N_{1/2}$ , a sort of “half life” for the stones during lithotripsy. That is, a stone will require  $N_{1/2}$  SWs for half of it to break away, and then another  $N_{1/2}$  SWs for half again to break away (leaving one quarter of the original stone). Thus, 97% of the stone would be eroded away at  $5 \times N_{1/2}$ . For these small cystine stones (4–7 mm), this  $5N_{1/2}$  value was 115 SWs for the stones showing void regions and 212 SWs for the stones appearing to be homogeneous by helical CT ( $P < 0.001$ ).

Both average and minimum values for CT number (in Hounsfield units, HU) correlated with SW/g to comminution ( $P < 0.003$  and  $P < 0.0003$ , respectively). Using the median value of average HU as a cutoff, the two groups were clearly different in fragility to SWs (Fig. 4). These groups also correlated with the CT observations, such that 10 of the 13 stones, with average HU values below the median, had been graded as containing visible internal

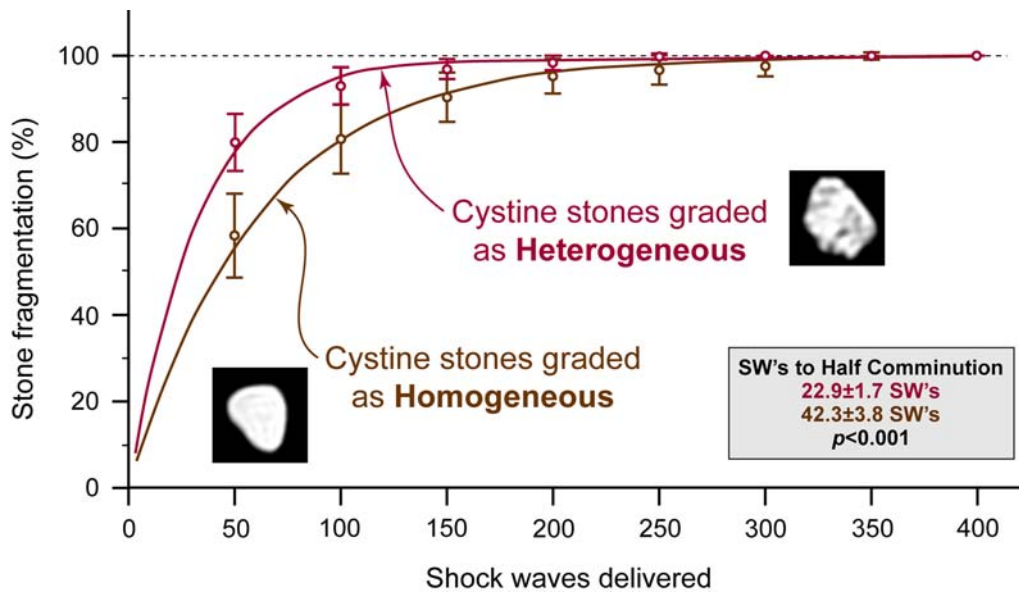


**Fig. 3** Comparison of breakage of cystine stones using nonlinear fitting. Stones are grouped as in Figs. 1, 2. SWs to half comminution show estimated value  $\pm$  approximate standard error

voids, while 9 of the 13 stones with average HU values above the median were also from the homogeneous group. Maximum values of HU did not show a positive correlation with SW/g to comminution; instead, these values were negatively correlated ( $P < 0.01$ ). This result can be explained by the effect of beam hardening artifact, seen in Fig. 1 as bright edges on some of the stones. Beam hardening (or “cupping” artifact) occurs because the lower energy portion of the X-rays is absorbed first, resulting in an apparently higher rate of absorption at the surface of an object [24]. In the homogeneous stones, the entire beam-hardening artifact is at the surface of the stones, so that the region-of-interest ellipse—drawn inside the edge of the stone—would not contain these bright edges. In the stones with internal voids, more of the beam hardening artifact appears within the body of the stone, and thus within the region-of-interest ellipse used for HU measurements.

Finally, the data collected here also confirm the basic observation of Bhatta et al., that rough cystine stones (having large crystals, and dark in color) break more easily than do smooth cystine stones (having fine crystals, and light in color). Rough cystine stones required only  $609 \pm 244$  SW/g ( $n = 11$ ) to comminution, smooth stones  $1,109 \pm 308$  SW/g ( $n = 8$ ), and stones intermediate in morphology  $869 \pm 384$  SW/g ( $n = 7$ ). Using the Tukey–Kramer HSD test, rough stones were different from smooth ( $P < 0.005$ ). Using nonlinear fitting to these morphological groups, smooth stones required more SWs than did stones classed as intermediate or rough ( $P < 0.001$ ), and intermediate and rough stones did not differ. SWs to half-comminution measured  $64 \pm 5$  for smooth stones,  $22 \pm 2$  for intermediate, and  $17 \pm 2$  for rough stones (all  $\pm$  approximate standard error).

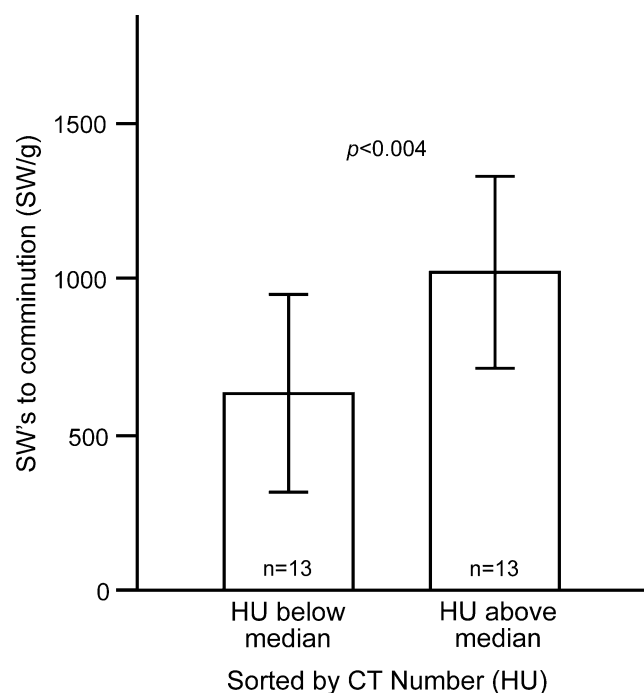


**Fig. 4** Comparison of fragility of cystine stones grouped by average CT number, in Hounsfield units. These groups did not differ in stone size, being  $5.4 \pm 0.9$  and  $5.8 \pm 0.9$  mm in diameter (below median and above median, respectively)

## Discussion

The data of Bhatta et al. [14], showing a difference in fragility between cystine stones of differing morphology, have been widely cited in the stone literature, even though only four stones—two rough and two smooth—were

included in their study. The present data, based on a larger number of stones, amply confirm their observation. The result makes intuitive sense, in that one would expect a stone composed of large crystals loosely held together to break more easily than one made of more closely packed, finer crystals.

However, the surface morphology of cystine stones cannot be observed in the patient. A method to determine stone roughness—using laser light scattering—has been demonstrated *in vitro* [15], but never implemented clinically. On the other hand, cystine stones with rough morphology also tend to contain internal void regions, which are detectable using clinical CT systems [17].

The present study demonstrates that classifying cystine stones by helical CT visualization of internal void regions successfully separates cystine stones that are relatively easy to break with SWs from those that are more resistant. This linkage of CT-visible structure with fragility to SWs opens the possibility that treatment decisions for cystine stones could include the structural characteristics of the stones, as observed by helical CT. This result also fits with that already reported for calcium oxalate monohydrate stones, in which stones with CT-visible internal structure were found to be more fragile than those with homogeneous appearance by helical CT [22].

The data in the present study also show that CT number, or Hounsfield units, of cystine stones correlate with resistance to breakage by SWs. However, this observation must be seen in the context of this study, in which the sizes of stones was tightly controlled (4–7 mm). The HU value measured on stones is highly correlated with stone size, and this artifact can lead to confusion if it is not considered carefully [25, 26]. Moreover, recent work has shown that HU value does *not* correlate with SW resistance in stones composed of calcium oxalate monohydrate [22]; so, the HU-fragility relationship seen with cystine stones certainly is not one that is universal among urinary calculi.

Additionally, it should be borne in mind that the present study was done *in vitro*, and utilized stones that were rather small (4–7 mm) compared with those that typically would be treated clinically. This has several ramifications for interpretation. The *in vitro* nature of the study means that the lithotripsy treatment of these stones was perfect—without any influences of target motion or coupling, both of which can reduce the effectiveness of lithotripsy treatment in the patient [27, 28]. The small size of these test stones also means that they were within the focus of the lithotripter shock wave, which would also enhance stone comminution [29]. Treatment of larger stones—or the use of a lithotripter with narrow focus—would likely result in poorer stone comminution. Finally, it should be noted that the imaging slice width used in the present study for helical CT (1.25 mm) is finer than that typically used clinically; in

the present study, this provided a good match for the small size of the test stones used, but extrapolation to larger stones imaged with coarser slice widths is not obvious, and actual observations *in vivo* will be required to ascertain if the structural features utilized in the present study can be differentiated in patients.

In conclusion, the present study confirms the hypothesis that CT-visibility of void regions in cystine stones is an indicator of fragility in SWL. Conversely, cystine stones that appear to be homogeneous by CT are likely to be resistant to SWs.

**Acknowledgments** Thanks to Molly Jackson for help with the stone fragmentation experiments, and to Dr. Robert Nadler and Dr. Edwin Prien for donating cystine stones from their collections. This work was supported by NIH R01 DK59933 and P01 DK43881.

## References

1. Harada M, Ko ZR, Kamidono S (1992) Experience with extracorporeal shock-wave lithotripsy for cystine calculi in 20 renal units. *J Endourol* 6:213–215
2. Martin X, Salas M, Labeeuw M, Pozet N, Gelet A, Dubernard JM (1991) Cystine stones: the impact of new treatment. *Br J Urol* 68:234–239
3. Kachel TA, Vijan SR, Dretler SP (1991) Endourological experience with cystine calculi and a treatment algorithm. *J Urol* 145:25–28
4. Katz G, Shapiro A, Lencovsky Z, Caine M, Pode D (1990) Place of extracorporeal shock-wave lithotripsy (ESWL) in management of cystine calculi. *Urology* 36:124–128
5. Hockley NM, Lingeman JE, Hutchinson RN (1989) Relative efficacy of extracorporeal shock wave lithotripsy and percutaneous nephrostolithotomy in the management of cystine calculi. *J Endourol* 3:273–285
6. Singer A, Das A (1989) Cystinuria: a review of the pathophysiology and management. *J Urol* 142:669–673
7. Hernandez-Graulau JM, Casteneda-Zuniga W, Hunter D, Hulbert JC (1989) Management of cystine nephrolithiasis by endourologic methods and shock-wave lithotripsy. *Urology* 34:139–143
8. Conort P, Leo JP, Richard F, Chatelain C (1989) Cystinic lithiasis and extracorporeal lithotripsy. *Ann Urol (Paris)* 23:253–254
9. Dretler SP (1988) Stone fragility—a new therapeutic distinction. *J Urol* 139:1124–1127
10. Newman DM, Lingeman JE, Mertz JH, Mosbaugh PG, Steele RE, Knapp PM Jr (1987) Extracorporeal shock-wave lithotripsy. *Urol Clin North Am* 14:63–71
11. Ng CS, Strem SB (2001) Medical and surgical therapy of the cystine stone patient. *Curr Opin Urol* 11:353–358
12. Trinchieri A, Montanari E, Zanetti G, Lizzano R (2007) The impact of new technology in the treatment of cystine stones. *Urol Res* 35:129–132
13. Daudon M, Bader CA, Jungers P (1993) Urinary calculi: review of classification methods and correlations with etiology. *Scanning Microsc* 7:1081–1106
14. Bhatta KM, Prien EL Jr, Dretler SP (1989) Cystine calculi—rough and smooth: a new clinical distinction. *J Urol* 142:937–940
15. Thibert R, Dubuc B, Dufour M, Tawashi R (1993) Evaluation of the surface roughness of cystine stones using a visible laser diode scattering approach. *Scanning Microsc* 7:555–560

16. Miller NL, Lingeman JE (2007) Management of kidney stones. *BMJ* 334:468–472
17. Kim SC, Hatt EK, Lingeman JE, Nadler RB, McAteer JA, Williams JC Jr (2005) Cystine: helical computerized tomography characterization of rough and smooth calculi in vitro. *J Urol* 174:1468–1471
18. Zarse CA, McAteer JA, Sommer AJ, Kim SC, Hatt EK, Lingeman JE, Evan AP, Williams JC Jr (2004) Nondestructive analysis of urinary calculi using micro computed tomography. *BMC Urol* 4:15
19. Williams JC Jr, Paterson RF, Kopecky KK, Lingeman JE, McAteer JA (2002) High resolution detection of internal structure of renal calculi by helical computerized tomography. *J Urol* 167:322–326
20. Saw KC, McAteer JA, Monga AG, Chua GT, Lingeman JE, Williams JC Jr (2000) Helical CT of urinary calculi: effect of stone composition, stone size, and scan collimation. *AJR Am J Roentgenol* 175:329–332
21. Cleveland RO, Bailey MR, Fineberg NS, Hartenbaum B, Lokhandwalla M, McAteer JA, Sturtevant B (2000) Design and characterization of a research electrohydraulic lithotripter patterned after the Dornier HM3. *Rev Sci Instrum* 71:2514–2525
22. Zarse CA, Hameed TA, Jackson ME, Pishchalnikov YA, Lingeman JE, McAteer JA, Williams JC Jr (2007) CT visible internal stone structure—but not Hounsfield unit value—of calcium oxalate monohydrate (COM) calculi predicts lithotripsy fragility in vitro. *Urol Res* 35:201–206
23. McAteer JA, Williams JC Jr, Cleveland RO, Van Cauwelaert J, Bailey MR, Lifshitz DA, Evan AP (2005) Ultracal-30 gypsum artificial stones for research on the mechanisms of stone breakage in shock wave lithotripsy. *Urol Res* 33:429–434
24. Kachelriess M, Sourbelle K, Kalender WA (2006) Empirical cupping correction: a first-order raw data pre-correction for cone-beam computed tomography. *Med Phys* 33:1269–1274
25. Williams JC Jr, Zarse CA, Jackson ME, Lingeman JE, McAteer JA (2007) Using helical CT to predict stone fragility in shock wave lithotripsy (SWL). In: Evan AP, Lingeman JE, Williams JC Jr (eds) *Renal stone disease: proceedings of the 1st international urolithiasis research symposium*. American Institute of Physics, Melville
26. Krishnamurthy MS, Ferucci PG, Sankey N, Chandhoke PS (2005) Is stone radiodensity a useful parameter for predicting outcome of extracorporeal shockwave lithotripsy for stones  $\leq 2$  cm? (Discussion 9) *Int Braz J Urol* 31:3–8
27. Cleveland RO, Anglade R, Babayan RK (2004) Effect of stone motion on in vitro comminution efficiency of a Storz Modulith SLX. *J Endourol* 18:629–633
28. Pishchalnikov YA, Neucks JS, VonDerHaar RJ, Pishchalnikova IV, Williams JC Jr, McAteer JA (2006) Air pockets trapped during routine coupling in dry head lithotripsy can significantly decrease the delivery of shock wave energy. *J Urol* 176:2706–2710
29. Sapozhnikov OA, Maxwell AD, MacConaghy B, Bailey MR (2007) A mechanistic analysis of stone fracture in lithotripsy. *J Acoust Soc Am* 121:1190–1202